Article details

Abdolahpur Monikh F., Grundschober N., Romeijn S., Arenas-Lago D., Vijver M.G., Jiskoot W & Peijnenburg W.J.G.M. (2019), Development of methods for extraction and analytical characterization of carbon-based nanomaterials (nanoplastics and carbon nanotubes) in biological and environmental matrices by asymmetrical flow field-flow fractionation, Environmental Pollution 255(2): 113304.
Doi: 10.1016/j.envpol.2019.113304

Environmental Pollution 255 (2019) 113304

Contents lists available at ScienceDirect

Environmental Pollution

journal homepage: www.elsevier.com/locate/envpol

Development of methods for extraction and analytical characterization of carbon-based nanomaterials (nanoplastics and carbon nanotubes) in biological and environmental matrices by asymmetrical flow field-flow fractionation☆

Fazel Abdolahpur Monikh [a, *], Nadine Grundschober [a], Stefan Romeijn [b], Daniel Arenas-Lago [c], Martina G. Vijver [a], Wim Jiskoot [b], Willie J.G.M. Peijnenburg [a, d]

[a] Institute of Environmental Sciences (CML), Leiden University, P.O. Box 9518, 2300 RA, Leiden, the Netherlands
[b] Division of BioTherapeutics, Leiden University, Leiden, the Netherlands
[c] Department of Plant Biology and Soil Science, University of Vigo, As Lagoas, Marcosende, 36310, Vigo, Spain
[d] National Institute of Public Health and the Environment (RIVM), Center for Safety of Substances and Products, Bilthoven, the Netherlands

ARTICLE INFO

Article history:
Received 19 July 2019
Received in revised form
23 September 2019
Accepted 24 September 2019
Available online 26 September 2019

Keywords:
Asymmetrical flow field-flow-fractionation
Multi-angle light scattering
Size distribution
Separation
Digestion

ABSTRACT

Suitable methods and fit-for-purpose techniques are required to allow characterization of carbon-based nanomaterials (CB-NMs) in complex matrices. In this study, two methods were developed; a method for extraction and characterization of CB-NMs in biological media and a method for fractionation of natural organic matter (NOM) coated CB-NMs in environmental matrices. The former method was developed by extracting carbon nanotubes (CNTs: sized 0.75 × 3000 nm) and nanoplastics (sized 60, 200 and 600 nm) from eggshells and characterizing the extracted CB-NMs in terms of particle size distribution using asymmetrical flow field-flow fractionation (AF4) coupled with multi-angle light scattering (MALS). The latter method was developed using AF4-MALS to fraction NOM-coated CNT (sized 0.75 × 3000 nm) and nanoplastics (sized 60, 200 and 300 nm) in a simulated natural surface water and provide information about the size distribution of the CB-NM-NOM complexes. The developed AF4-MALS method successfully fractioned the CB-NM-NOM complexes based on hydrodynamic size and provided the size distribution of the complexes. The NOM corona did not shift significantly the median size of the CB-NMs. It influenced however the size distribution of the nanoplastics and CNTs. The sample preparation method failed to extract the CNTs (recovery < 20%) from the matrices of the eggshells while being successful for extracting the nanoplastics (recoveries > 60%). The AF4-MALS fractogram showed that the extraction method did not significantly influence the size distribution of the nanoplastics of 60 and 200 nm size, whereas the peak of 600 nm nanoplastics shifted towards a smaller hydrodynamic size. In conclusion, the developed sample preparation method followed by the developed AF4-MALS method can be applied for extraction, separation and characterization of CB-NMs in biological and environmental matrices. Thus, the methods have a high potential to be methods of choice to investigate CB-NMs in future studies.

1. Introduction

The progress of nanotechnology has led to the synthesis and production of nanomaterials (NMs) with diverse chemical composition and specific size and/or surface characteristics. As one class of extensively produced NMs, carbon-based (CB)-NMs such as carbon nanotubes (CNTs) exhibit a broad range of potential application such as optical biosensors, drug delivery systems, and electronic composites (Benito et al., 2015; Maser et al., 2002; Tapasztó et al., 2005). Another class of emerging CB-NMs are nanoplastics (defined on the basis of their diameter being < 1000 nm). Nanoplastics are mostly released unintentionally from macro and microplastics in the environment due to degradation and fragmentation of plastic upon aging (Gigault et al., 2018; Ter Halle et al.,

☆ This paper has been recommended for acceptance by Baoshan Xing.
* Corresponding author. Van Steenis Building, Einsteinweg 2, 2333 CC, Leiden, the Netherlands.
E-mail address: f.a.monikh@cml.leidenuniv.nl (F. Abdolahpur Monikh).

https://doi.org/10.1016/j.envpol.2019.113304
0269-7491/

2016; Lambert and Wagner, 2016), so-called secondary nanoplastics. The exponential growth of CB-NMs applications and their release into the environment has led to the increasing concern on their adverse environmental effects (Li and Martin, 2016).

The fate of CNTs and nanoplastics in aquatic systems can be influenced by hydro-chemical parameters of the system, such as pH, the concentration of electrolytes, and the concentration and type of natural organic matter (NOM) (Freixa et al., 2018). NOM consists of a heterogeneous mixture of humic substances, hydrophilic acids, proteins, etc., derived from degradation of plants and animal residues in waterbodies (Hong and Elimelech, 1997). NOM can attach to the surface of NMs, forming so-called NOM corona and inducing a negative surface charge as well as steric stabilization to the particles (Arenas-Lago et al., 2019a; Arenas-Lago et al., 2019b). Thus, the characterization of NM-NOM complexes is important for fate assessment of the CB-NMs.

CNTs can persist for a long time in the environment (Garner and Keller, 2014) and may enter organisms (Cano et al., 2018). Although CNTs can be ingested by organisms, absorption across epithelial surfaces is limited, thus, systemic distribution of CNTs is unlikely. It was documented that due to their persistence in the environment, plastics fragments can accumulate in organisms (Nelms et al., 2018; Welden et al., 2018; Au et al., 2017; Macali et al., 2018). The surface properties of CNTs and nanoplastics are roughly similar to the properties of persistent organic pollutants (POPs) in terms of hydrophobicity (Eatemadi et al., 2014; Cole et al., 2011; Crawford and Quinn, 2016). Thus, they may have a similar fate as POPs in some organisms. For example, previous studies have documented that eggs are useful tissues samples for monitoring POPs because females birds can excrete the contaminants in their eggs and eggshells (Fimreite et al., 1982; Gochfeld and Burger, 1998). For many birds, eggs can thus serve as bioindicators of internal contamination (Fimreite et al., 1982; Cole et al., 2011). This has not been documented for nanomaterials, which could be due to limitations in analytical techniques.

The sluggish movement in understanding CB-NMs fate and adverse effects compared to other types of NMs or macroplastics stems from the limitation in methods and techniques that are capable of characterizing CB-NMs in complex matrices (Abdolahpur Monikh et al., 2019). Characterization of nanoplastics and CNTs in biological and environmental matrices is even more challenging due to the presence of other biological molecules and background carbon-based materials which may interfere with the characterization of the NMs of interest (Petersen et al., 2016). CB-NMs have high free surface energy causing the thermodynamic driving forces to minimize the surface energy through different chemical and physical reactions, like aggregation, dissolution and/or ligand adsorption (Bogatu and Leszczynska, 2016; Navrotsky, 2010; Westerhoff et al., 2013). Thus, in a dispersion of CB-NMs, one may encounter single particles and aggregates. The occurrence of nanoplastics and CNTs in different size distributions hinders the application of many available techniques. Some techniques such as transmission electron microscopy (TEM) are commonly used to characterize NMs (Abdolahpur Monikh et al., 2019). However, TEM has some disadvantages in terms of expense, complexity and sample preparation, which makes it less suitable for undertaking routine measurements (Calzolai et al., 2012). Nanoparticle tracking analysis (NTA) and dynamic light scattering (DLS) are moderately priced techniques and able to assess large amounts of particles in a sample without the requirement for tedious sample preparation methods. However, the direct measurement of polydisperse NM samples using NTA and DLS is problematic (Domingos et al., 2009; Abdolahpur Monikh et al., 2019).

Asymmetrical flow field-flow fractionation (AF4) represents a flow-based separation methodology using a separation channel where the retention and separation are caused by an external field (so-called crossflow). The theory behind AF4 and the mechanisms of functioning have been well described in the literature (Giddings et al., 1976). AF4 can be used for the analysis of NMs in liquid matrices. For example, Loeschner et al. (2015), Wagner et al. (2015) and López-Heras et al. (2014), separated NMs from consumer products using AF4 and reported that this technique is a powerful tool to achieve information about the size distribution of NMs in complex matrices. AF4 was also reported to be an ideal tool to divide CNTs with broad size distributions into discrete, roughly monodisperse fractions for further characterization (Moon et al., 2004).

Thus, the first objective of this study was to develop a sample preparation method for extraction of CNTs and nanoplastics from eggshells with minimum influence on the particles size distribution and characterize the extracted particle in terms of size distribution using AF4-MALS. The second objective was to develop a AF4-MALS method to fraction CB-NM-NOM complexes based on size in a simulated natural water samples and elucidate the influence of the NOM corona on the size distribution of CNTs and nanoplastics.

2. Materials and methods

2.1. Materials

All water was deionized by reverse osmosis and purified by a Millipore Milli-Q (MQ) system. The single-walled CNTs were purchased from Sigma Aldrich (St. Louis, USA). The diameter and median length of the CNTs were 0.75 nm and 3 μm, respectively. Spherical polystyrene nanoparticles of 60 nm, 200 nm, 300 nm and 600 nm diameter size were purchased from ThermoFisher Scientific (Waltham, USA). Suwannee River NOM was supplied by the International Humic Substances Society (1R101N). Eggs were purchased from a local farm in the Netherlands. Sodium dodecyl sulfate (SDS) was provided from Sigma Aldrich (the Netherlands). Hydrochloric acid (30%) and sodium hydroxide (NaOH) were of analytical grade and purchased from Merck, Germany. Sodium chloride (NaCl) of analytical grade and tetramethylammonium hydroxide (TMAH; 20%) were obtained from Sigma-Aldrich, the Netherlands. The carrier solutions used for AF4 analyses were filtered before use (Anodisc < 0.1 μm filter, Whatman, Maidstone, UK). Preparation of NOM suspension is described in Section 1 of the Supporting Information (SI).

2.2. Characterization of the pristine nanoplastics and CNTs

Preparation of the NM dispersions is reported in Section 2 (SI). Dynamic light scattering was used to measure the hydrodynamic size of the nanoplastics on a Zetasizer Nanodevice (Malvern, the Netherlands). The same instrument was used for measuring the zeta potential of the CNTs and nanoplastics by laser Doppler electrophoresis. TEM (JEM-1400, the Netherlands) was used to visualize the NMs and characterize the particles in terms of projected size and shape. NTA (NanoSight's NS200, Malvern, the Netherlands) was used to measure the size and number concentration of the nanoplastics.

2.3. Incubation of the CNTs and nanoplastics in a suspension of NOM

The influence of formation of a NOM corona on the size distribution of CNTs and nanoplastics was investigated. The CNTs or nanoplastics (60, 200 and 300 nm) were dispersed separately in NOM suspension and diluted with MQ water to reach a final

concentration of 50 mg/L of the NMs and 10 mg/L of NOM in the dispersions. The dispersions were incubated at 4 °C for 1 h. This concentration of the NMs was selected to meet the limitation of the AF4-MALS. The NOM concentration was selected because it represents an average of a realistic NOM level in natural surface water (Abdolahpur Monikh et al., 2018b). After incubation, the sample was used for characterization.

2.4. Extraction of the particles from the biological media

The sample preparation followed the generic scheme suggested by Abdolahpur Monikh et al. (2019) for the extraction of CB-NMs from biological media. As illustrated in Fig. 1, the scheme is based on a stepwise approach starting with washing (Step 1), followed by digestion (Step 2), purification (Step 3), enrichment (Step 4) and stabilization (Step 5). The extracted particle suspension was subsequently separated using AF4 with regard to size distribution and detected by MALS (Step 6). The sample preparation method aims at the separation of the CNTs and nanoplastics from the background matrix of the eggshells (used as a generally available model of biological media) with minimum alteration in the size distribution of the CNTs and the particles. The sample preparation was as follows; the eggshells (without separating the proteins layer inside the eggshells) were washed three times using MQ water and dried at 60 °C in an oven for 2 h. The eggshells were powdered and dried further at 60 °C in an oven for 1 h. One gram of the resulting eggshells powder was dispersed in MQ water with pH 9.5 and stirred using a magnet for 5 h. During the stirring process (after 30 min of stirring), immediately after sonication aliquots of the stock nanoplastics (10 g/L) or CNTs (10 g/L) dispersions were spiked to the eggshells dispersion to reach a final concentration of 100 mg/L of the CNTs or nanoplastics, allowing the NMs to interact with the eggshells particles. The selected pH 9.5 facilitates the degradation of the stabilizer agents on the surface of the pristine NMs (Abdolahpur Monikh et al., 2019), thus enhance the attachment of the NMs to the eggshells particles. Ten mM of Ca^{2+} was added to the dispersions of nanoplastics to further enhance the interaction of the eggshells particles with the nanoplastics because this Ca^{2+} concentration increases the zeta potential of nanoplastics toward less negative values (-7 ± 4), regardless of the particle size. After stirring, the samples were left for one day at room temperature to allow further interaction of the particles with the eggshells. After 24 h of interaction and sedimentation, the pellets were separated and the supernatants were removed. We assumed that most of the NMs are attached to the eggshell particles. The pellets were washed with MQ waters for two times to remove the NMs that are not bound to the eggshells. After washing, we imaged the nanoplastics attached to the eggshells particles using TEM (Figs. S1 and SI). The residuals were dispersed in 100 ml of MQ water and digested using HCl (0.01 M) at 50 °C for 2 h to dissolve the eggshells and release the attached particles from the eggshell particles. The digestion was smoothly carried out at pH 4.5 to minimize any influence of the acid and temperature on the NMs of interest. After 2 h, the residuals were kept at room temperature (at pH = 4.5) for 5 days to further dissolve the $CaCO_3$ layer of the eggshells. The pH of the dispersion was adjusted to 4.5 twice a day. After 5 days, all the organic

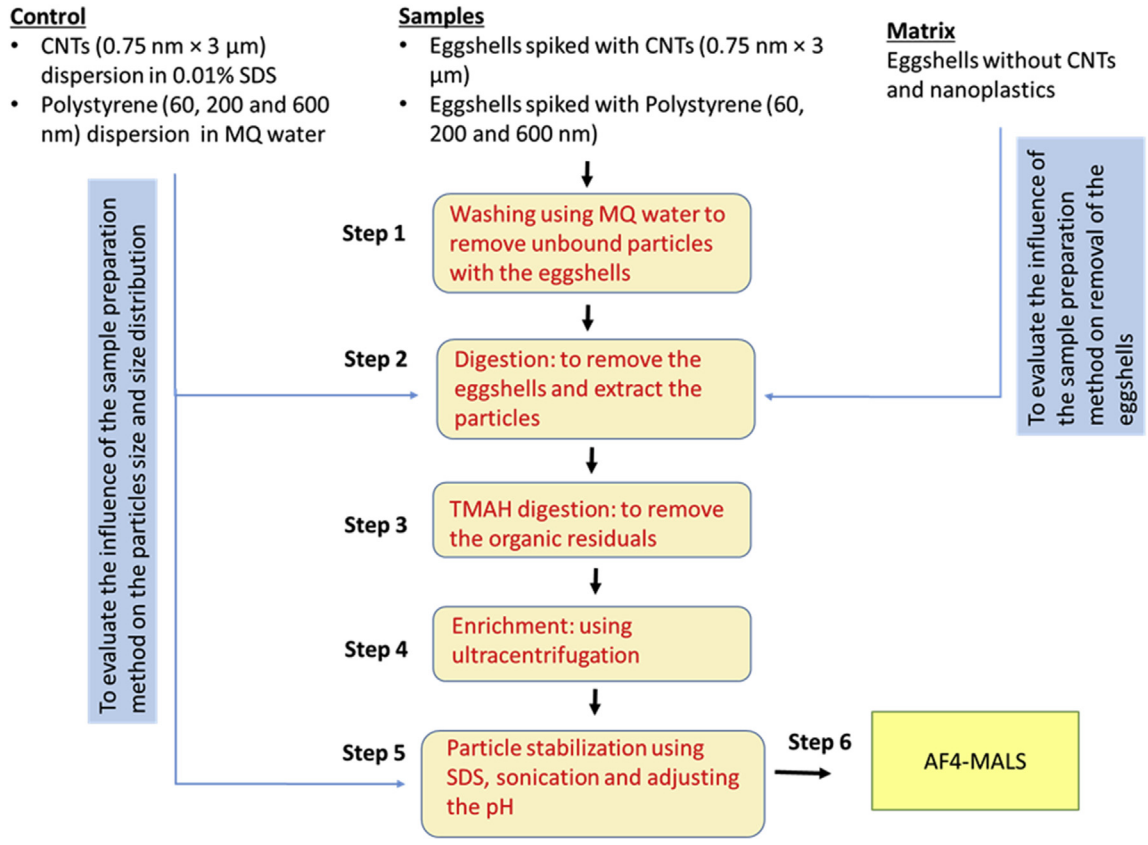

Fig. 1. Sample preparation procedures used to extract the nanoplastics and the CNTs from the eggshells. The control samples (containing the nanoplastics particles in MQ water and the CNTs in 0.01% SDS dispersion) were treated using the extraction method. The obtained data for CB-NMs after treatment were compared with the data obtained for the same CB-NMs before treatment. This allowed us to evaluate the influence of the extraction method on the particles size and size distribution. The matrix sample (control samples contain eggshells without any added CB-NMs) was treated using the same extraction method to evaluate whether the method can remove the background matrices of the eggshells and isolate the particles.

materials which were not digested during the acid digestion process, were dissolved using 5% TMAH solution at 60 °C for 1 h. The concentration of the extracted NMs in the samples should be high enough to be separated by AF4 and detected by MALS. Thus, the samples were enriched (step 4) using an ultracentrifuge (Beckman Coulter, Optima L-90 K) at 40000 rpm (Fixed-Angle Rotor, Titanium: 25^0, $rpm_{max} = 90000$, $g_{max} = 694000$, tube volume 13.5, rotor capacity 108 ml) for 20 min.

We expect that the sample preparation also removed or altered any stabilizing compound which was adsorbed to the surface of the pristine NMs. Thus, before injecting the extracted nanoplastics and CNTs into the AF4, the NMs need to be stabilized to prevent agglomeration and aggregation (Abdolahpur Monikh et al., 2019). Selecting a suitable dispersant is of paramount importance in the sample preparation method to achieve a stable dispersion. In the stabilization part (step 5), the separated particles were stabilized using SDS (0.01%) and sonicated for 10 min with a bath sonicator (40 W in 15 ml volume). The pH value of the samples was adjusted to 8–8.5 using 10 mM NaOH solutions. These alkaline conditions improve the particle stability by shifting the surface potential of all involved NMs to negative values. The zeta potential of the particles before and after stabilization was measured. To evaluate whether the developed sample preparation method can successfully remove the background matrices of eggshells, a control sample (matrix sample) (Fig. 1) containing only the eggshells without any additives were run along with the samples.

The sample preparation process may influence the NMs and may lead to particle agglomeration and/or degradation (Abdolahpur Monikh et al., 2018a). Possible alterations in the particle size distribution of the NMs due to the sample preparation method were evaluated by comparing the size distribution of the pristine particles before the sample preparation process with the size distribution of the particles after sample preparation. Accordingly, we used control samples which contained the dispersion of the nanoplastics in MQ water or CNTs in 0.01% SDS solution.

2.5. AF4-MALS

An AF4 system coupled on-line with a UV–Vis detector and a MALS detector was used to characterize the size distribution of different NMs and the molecular weight of the NOM. The AF4 system was coupled online with an 18 angle MALS detector and a linear polarized laser at 658 nm (DAWN® EOS™, Wyatt Technology Europe GmbH, Dernbach, Germany). The data acquisition interval was set to 8 s. Polystyrene particles (60, 200 and 300 nm) were used as reference particles to investigate the performance of the AF4 following the method reported by (Hawe et al., 2012). The mass of the injected particles was equal to 50, 25 and 10 mg/L, respectively, to match the size-dependent sensitivity of the MALS detector. In all the methods, an injection flow of 0.2 mL/min was applied if not stated otherwise. An injection volume of 50 μL was used. The MALS detector determined the size distribution of the particles based on light intensity. Calibration of the AF4 was performed under similar run conditions. The root mean square radius (R_{rms}) was derived from MALS measurements with the Zimm (for nanoplastics of 60 nm) (Wagner et al., 2015) or Debye fit (for 200, 300 and 600 nm nanoplastics) method (Hupfeld et al., 2009). After each run, the channel was washed using MQ water or SDS solution. In order to reduce the bacterial growth in the channel, sodium azide 0.025% in MQ water was running overnights and weekends.

2.6. Characterization of the molecular weight of NOM using AF4-MALS

NOM can be separated into different fractions using AF4, as based on molecular weights of the compounds forming the NOM. A suspension of NOM with a concentration of 250 mg/L was analysed using 10 mM NaCl and Triton X-100 (0.002%) as a carrier liquid. The developed AF4 method for fractionation of the NOM is reported in Table S2 (SI).

2.7. Characterization of nanoplastics and CNTs using AF4-MALS

To provide a suitable dispersant for the fractionation of CNTs and nanoplastics using AF4, two SDS concentrations of 0.01 and 1% in MQ water were used. The AF4 set up for fractionation of CNTs and nanoplastics in SDS dispersion, and NM-NOM complexes is reported in Table S2 (SI).

2.8. Data analysis

Astra software (software version 5.3.4.20 (Wyatt Technology Europe GmbH, Dernbach, Germany) was used to extract the R_{rms} from MALS. Based on the size calibration using polystyrene particles, the hydrodynamic diameter was calculated (Formula S1, SI). The calculation of the areas under the light scattering (LS) signals resulting from AF4-MALS and plotting of the fractograms were carried out in the software OrginLab 9.1. The AF4-MALS recovery (Formula S2), the total recovery (Formula S3) and the particle number recovery (Formula S4) calculation is described in Section 5 (SI). The AF4-MALS recovery allows us to estimate the amount of CB-NMs which was lost due to the separation using AF4, either through attachment to the membrane or to the tubing. The total recovery and particle number recovery allowed us to assess the amount of CB-NMs which was lost due to the sample preparation method (particles extraction).

3. Results and discussion

3.1. Characterization of the pristine CNTs and nanoplastics

Different experimental approaches were considered to improve the dispersion stability of the CNTs and nanoplastics; a) through functionalization of the particles with a suitable stabilizer (SDS and Triton X-100), b) through using a tip or bath sonicator, and c) through different sonication times (see Tables S1 and SI). Stabilization of CNTs was problematic due to their high free surface energy. The hydrodynamic size of the CNTs in MQ water could not be measured due to the fast agglomeration of the tubes, which makes using the DLS at typical operational time-scales challenging due to the limitation of DLS in measuring a dispersion with a high polydispersity (Abdolahpur Monikh et al., 2019). The CNTs were dispersed using SDS (10%) and tip sonication (40 W in 50 ml) for 10 min. The aggregates were not observable in the bottom of the container after 10 min. This dispersion was only used for CNTs characterization in terms of size using TEM.

CNTs and nanoplastics were imaged by TEM prior to sample preparation and after incubation in NOM suspension (Figs. S2 and SI). The TEM measured size for CNTs is reported in Table S3 (SI) and was in good agreement with the reported values by the supplier. The TEM picture for CNTs (Fig. S2a) showed that homoaggregation (agglomeration between particles of the same type) is not the only form of aggregation that occurs in CNTs dispersion, but self-agglomeration was found to take place where the head of the tubes attaches to the other part of the 'body' of the tubes, as can be seen in Figs. S2a and SI. The TEM pictures for the nanoplastics in MQ are shown in Figs. S2b–d (SI). The particles were spherical in shape and the measured size was in good agreement with the size reported by the supplier (Tables S3 and SI).

The zeta potential of the pristine nanoplastics particles and CNTs

was obtained by dispersing the particles in MQ water (Tables S3 and SI). Although it was problematic to provide a dispersion of the CNTs in MQ water, we carried out a quick measurement of the dispersion after 1 h of bath sonication to obtain the zeta potential. The data showed that the nanoplastics particles had a negative zeta potential, whereas the zeta potential of the CNTs was slightly positive (Tables S3 and SI). This can explain the very fast agglomeration of the CNTs, as previously reported (Koh and Cheng, 2014).

After incubation of NMs with NOM suspension, components from the NOM are adsorbed to the surface of the CNTs (Figs. S2e and SI) and the nanoplastics (Figs. S2f and SI). Although, the adsorption of NOM components to the surface of the CNTs decreased the zeta potential to −18 mV, but could not sufficiently stabilize the particles against agglomeration (Figs. S3a and SI). After attachment of NOM components to the surface of the nanoplastics, the zeta potential did not change significantly. The attachment of negative charged NOM to the surface of negative charged NMs occurs under specific interaction; meaning the surface charge of the particles may not prevent the NOM components (which are mostly negatively charged) from attaching to the surface of the particles (Abdolahpur Monikh et al., 2018b). Due to the high negative value of the zeta potential, the dispersions of the nanoplastics were stable over time as it was confirmed by measuring the aggregation kinetics of the nanoplastics over 30 min (Figs. S3b and SI).

3.2. Evaluation of the performance of the AF4

To evaluate the performance of the AF4, a mixture of polystyrene particles with three different particle sizes, 60, 200, and 300 nm, was analysed using the AF4-MALS. The fractogram is reported in Fig. S4 (SI) and shows a good separation of the particles based on their size. Fig. S4 (SI) confirms that the method is suited to provide the size distribution of the mixture of particles. The R_{rms} values show that the method can separate the particles according to the normal mode (not steric mode) of AF4 where the smaller particles are eluting before the larger particles (Beckett, 2005). The AF4-MALS recoveries for polystyrene dispersed in MQ water were higher than 80%. This means that most of the particles were eluted from the channel and a small percentage of particles were lost due to adsorption to the tubing or to the membrane (Schmidt et al., 2009; von der Kammer et al., 2011; López-Heras et al., 2014).

3.3. Separation of the pristine CNTs and nanoplastics in SDS dispersion

Since dispersing the CNTs in MQ water was not possible in our study, we stabilized the CNTs and the nanoplastics using 0.01% SDS for separation by AF4. It is reported that SDS is a compatible surfactant with the AF4 system (Beckett, 2005) and able to stabilize NMs for a long time (López-Heras et al., 2014). A stabilized dispersion of the NMs was separated using the AF4 to measure the size distribution of the particles and to use it as a standard to assess the influence of NOM corona and the sample preparation method on the size distribution of the NMs in the next sections.

The results for the CNTs are based on the equivalent spherical particle diameter calculated from the fractogram of the CNTs based on the normal AF4 theory (Chen and Selegue, 2002; Chun et al., 2008). The AF4-MALS fractogram of the CNTs dispersed in SDS solution is reported in Fig. S5a (SI). Three peaks were measured for the CNTs, which showed that there are three populations of CNTs in the samples. The distribution of CNTs is equivalent to a distribution of spherical particles with hydrodynamic diameters peak at 300, 400 and 600 nm. The obtained values of R_{rms} show that the populations with the peak at 300 and 400 nm eluted following the normal mode of AF4. The R_{rms} for 600 populations signal showed that steric transition might have happened. Steric mode of separation in AF4 occurs when the size of particles increase and, consequently, the diffusion coefficient decreases, thus, the separation sequence is inverted and the larger particles elute before the smaller particles (Kowalkowski et al., 2018). Similarly, Correia et al. (2018) reported that NMs extracted from complex matrices eluted following the steric separation when the particle size increased to larger than 300 nm. The measured size distribution of CNTs showed that the SDS could not totally stop the agglomeration between the tubes. Thus, the CNTs agglomerated and the agglomerates appears in three different populations. It is possible that the CNTs wrapped into coil-shaped bundles (self-agglomerate) and behaved similarly to spherical particles in the channel (Chen and Selegue, 2002). This phenomenon would, first, create a polydisperse sample and, second, complicate the measurement of the size of the tubes. It is highly possible that CNTs become entangled in the membrane under the relatively high pressures resulting from the cross flow of the AF4 (Chen and Selegue, 2002). The obtained recovery for the AF4-MALS (75%) confirms the loss of the CNTs during the fractionation.

The fractogram for the mixture of the nanoplastics is reported in Fig. S5b (SI). Three peaks were obtained for the nanoplastics, with a hydrodynamic diameter of around 65, 190 and 300 nm. The calculated recoveries were >80%, which showed that the loss of the particles due to the interaction between the membrane and the nanoplastics was low. The fractogram shows that the SDS does not influence the size distribution of the nanoplastics when compared to the fractogram of the pristine nanoplastics dispersed in MQ water (Figs. S4 and SI). The data showed that the developed method can separate the CNTs and the nanoplastics based on their hydrodynamic size and provide details about the size distribution of the stabilized CNTs and nanoplastics. Thus, we used the method for characterization of the CNTs and nanoplastics in the simulated surface water samples and the CNTs and nanoplastics extracted from the eggshells.

3.4. Separation of CNT-NOM and nanoplastics-NOM corona using AF4

To evaluate the ability of the developed method in the separation of the NM-NOM complexes and to investigate the influence of the NOM corona on the size distribution of the CNTs and nanoplastics, we first fractionated the NOM using the AF4. NOM is composed of many molecules with different molecular weight, which makes the characterization of the entire components of the NOM a challenging task (Zhou and Guo, 2015; Assemi et al., 2004; Moon et al., 2006). The obtained fractogram for the NOM suspension is shown in Fig. 2a. The highest peak was observed at the hydrodynamic size range between 300 and 600 nm. Some molecules were eluted at hydrodynamic lower than 300 nm, but with low intensity. We calculated a low AF4-MALS recovery for the NOM (<30%). It is likely that due to the cross flow force a considerable amount of the small molecules of the NOM suspension passed the membrane and only the fractions which have a size higher than the membrane cut-off reach the detector (Moon et al., 2006). A previous study reported a low recovery for NOM due to the application of a 10 kDa membrane (Zhou and Guo, 2015). It is also possible that the cross flow led to NOM attachment to the membrane, consequently, the NOM did not reach the MALS detector.

Many study have reported that NOM attaches to CNTs and nanoplastics to form an NOM corona on the surface of the particles (Yang and Xing, 2009; Lu and Su, 2007). But few studies were able to provide information on the size distribution of the CNT-NOM and nanoplastic-NOM complex. The developed AF4-MALS method was

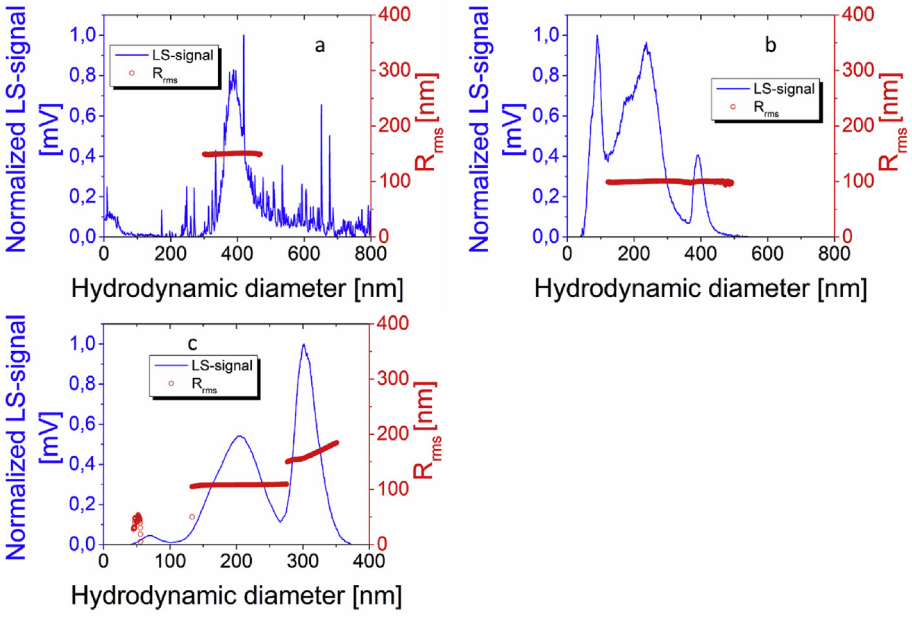

Fig. 2. AF4-MALS fractograms obtained for a) NOM suspended in MQ water and Triton X-100, b) CNT-NOM complex, and c) a mixture of 60, 200 and 300 nm nanoplastics incubated in NOM suspension for 1 h.

used to separate and characterize the CNT-NOM complexes in term of size distribution. The AF4-MALS fractogram for CNT-NOM is shown in Fig. 2b. The fractogram of the CNT-NOM was different compared to the fractogram of CNT stabilized by SDS (Figs. S4 and SI). The size distribution of the CNT-NOM complexes shifted toward a smaller hydrodynamic size. Clearly, the NOM corona influences the size distribution of the CNTs by increasing the intensity of the small populations in the samples compared to CNTs in SDS solution (Hyung et al., 2007). Since the NOM could not efficiently stabilize the CNTs, we expected that the CNTs agglomerate, to some extent, in the presence of NOM and the agglomerates would elute at larger hydrodynamic size. The higher intensity of smaller population could be related to the NOM compounds which were present in the samples. The calculated AF4-MALS recovery varied between 20 and 40% which is not surprising due to the expected high interaction between the membrane and the analytes due to the presence of NOM (Zhou and Guo, 2015).

The fractogram of the dispersion contains the mixture of nanoplastic (60, 200 and 300 nm) coated with NOM is shown in Fig. 2c. The developed method could fraction the nanoplastic-NOM complexes based on size and provide the size distribution of the particles-NOM complexes. The finding showed that NOM influences the size distribution of the nanoplastics but has a small influence on the median size because the nanoplastics-NOM complexes eluted at the same hydrodynamic diameter as the pristine nanoplastics. However, the intensity of the LS signals decreased in the peak of 60 nm nanoplastics-NOM compared to the fractogram of the nanoplastics in SDS. The peak of the 200 nm nanoplastic-NOM appeared to be wider than the peak obtained in case of 200 nm nanoplastics in SDS. It is possible that some of the 60 nm nanoplastics agglomerated to form particles with larger sizes which eluted with the 200 nm particles. It is possible that the NOM influences the diffusion of the particles in the channel and the interaction of the particles with the membrane. This was confirmed by the lower AF4-MALS recovery (40–55%) obtained for nanoplastic-NOM compare to nanoplastic-SDS and pristine nanoplastic in MQ water.

3.5. Characterization of CNTs and nanoplastics extracted from eggshells

The sample preparation method could not extract the CNTs from the eggshells with high total recoveries. Low AF4-MALS and total recovery was also measured for control CNTs (Table 1). Thus, the concentration of the CNTs in the samples, even after enrichment, was not sufficient to be separated by AF4 and detected by MALS. This unsuccessful extraction of the CNTs could be due to the influence of the method extraction processes on the CNT which could lead to particles removal or even degradation. Using a two-step extraction method of 2.5% sodium hydroxide/surfactant mixture and proteinase K, Doudrick et al. (2013) could obtain a recovery of 98% for CNTs from a rat lung. However, their approach is not suitable to destroy the inorganic structures of biological samples such as eggshells to extract NMs. Gogos et al. (2014) extracted CNTs from soil and quantified the extracted particles using AF4-MALS. Their approach too is not applicable for extracting CNTs from biological media and cannot isolate the particles from the matrix of eggshell. Accordingly, in this section, we focus only on the nanoplastics. We used nanoplastics of 60, 200 and 600 nm size to cover a broad size range of nanoplastics.

The total recovery, AF4-MALS recovery, and the size as well as zeta potential data of the nanoplastics in the control samples and the nanoplastics extracted from the eggshells are reported in Table 1. The nanoplastics were characterized in terms of hydrodynamic size and zeta potential after extraction. The stability of the particles against agglomeration was monitored using DLS analysis (before injection to the AF4) to ensure that the particles are stable during the fractionation in the AF4 (Figs. S6 and SI). We defined the stability of the samples by means of the measured agglomeration kinetics (change in the hydrodynamic diameter directly after sonication) during 30 min. Regarding the control nanoplastics, the calculated AF4 recoveries were between 73% and 85% and the total recoveries were between 62% and 67% (Table 1). Our particle extraction method showed high recovery compared to a previous method where a solution of 35% HNO_3 melded and dissolved some

Table 1
Recoveries, size distribution and zeta potential of CNTs (control) and nanoplastics (60, 200, 600 nm; controls and extracted from eggshells).

Sample	AF4-MALS recovery [%]	Total recovery [%]	Particle number recovery [%]	AF4 measured median (MALS) nm	DLS measured Z-average diameter (nm)	Zeta potential before stabilization	Zeta potential after stabilization
Control CNTs	<25	<25	–	–	–	4 ± 2	−26 ± 5
Control nanoplastics 60 nm	73 ± 5	63 ± 5	58 ± 3	48 ± 4	112 ± 23	−17 ± 6	−52 ± 4
Control nanoplastics 200 nm	85 ± 8	62 ± 4	54 ± 4	168 ± 9	314 ± 56	−15 ± 3	−49 ± 5
Control nanoplastics 600 nm	76 ± 4	67 ± 12	57 ± 6	623 ± 17	854 ± 123	−16 ± 2	−50 ± 3
Extracted 60 nm nanoplastics	81 ± 7	71 ± 10	63 ± 5	47 ± 3	98 ± 18	−16 ± 4	−48 ± 5
Extracted 200 nm nanoplastics	74 ± 4	60 ± 6	54 ± 7	170 ± 5	279 ± 83	−16 ± 3	−49 ± 2
Extracted 600 nm nanoplastics	79 ± 6	64 ± 11	60 ± 9	485 ± 12 and 549 ± 23	765 ± 73	−14 ± 5	−48 ± 4

plastic particles (Avio et al., 2015; Catarino et al., 2017; Dehaut et al., 2016). Application of an acidic mixture of HNO_3 and $HClO_4$ led to complete dissolution of the plastic particles (Enders et al., 2017).

The AF4-MALS recoveries and the total recoveries for extracted nanoplastics from the eggshells were between 74%-84% and 60%–71%, respectively (Table 1). The obtained AF4-MALS recoveries showed that a high percentage of the particles were recovered without being lost during the separation in the AF4. The total recovery showed that, although some of the particles were lost due to the sample preparation method, a high percentage of the particles were successfully (with high recovery) extracted from the eggshells. This was also confirmed by the number of particles measured after the extraction as compared to the number of particles before extraction using NTA (Table 1). There are no AF4 data available for nanoplastics in the literature. However, the calculated AF4-MALS recovery was similar to that reported for titanium dioxide NMs (82%) by Peters et al. (2014) and (80%) Abdolahpur Monikh et al. (Abdolahpur Monikh et al., 2018a).

We evaluated whether the sample preparation methods for NMs extraction influenced the size distribution of the separated particles. The DLS-measured particle sizes of the control and extracted nanoplastics (Table 1) were compared to the DLS-measured pristine particles size (Tables S3 and SI). The results showed that the measured size of the control and extracted nanoplastics were larger than those of pristine particles. These increases in the hydrodynamic size of the particles could be due to the attachment of the stabilizer to the surface of the particles after step 5 of the sample preparation method (López-Miranda et al., 2012). The zeta potential of the particles changed towards a less negative value after the extraction of the particles. After the stabilization of the extracted particles and adjustment of the pH (step 5), the zeta potential was found to be more negative (Table 1).

The particle size distributions of the control and the extracted nanoplastics are presented in Fig. 3. No peak was observed for the matrix samples (eggshells without NMs). This indicated that the sample preparation method can remove the matrix of the eggshells. The obtained fractograms and calculated R_{rms} for the control sample (Fig. 3a,c,e) were similar to those of the pristine nanoplastics. However, the peaks shifted toward smaller hydrodynamic size. The size distribution of the 60 nm was slightly wider in the control sample compared to the size distribution of the same particle in MQ water. The fractogram of 200 nm particles showed a peak at around 168 nm (hydrodynamic size) and a tail at a larger hydrodynamic size, indicating that the sample preparation method slightly decreased the size distribution of the 200 nm nanoplastics.

We compared the size distribution of the nanoplastics in the control samples with that of the extracted nanoplastics (Fig. 3a–f). A green dash was implemented in each fractogram (Fig. 3) to facilitate the comparison of the peaks of the extracted nanoplastics from those of the control nanoplastics. The gradual increase in R_{rms} over the hydrodynamic size span in most of the fractograms (Fig. 3) confirms that the fractionation occurred according to the normal mode of elution. The peak of the 60 nm control sample and the 60 nm extracted nanoplastics sample appeared at the same hydrodynamic diameter. The median hydrodynamic size also was similar between the control and extracted samples (Table 1). Similarly, the peak of the extracted 200 nm nanoplastics appeared at the same hydrodynamic size as the peak measured for the control 200 nm nanoplastics, with a hydrodynamic median size at around 168–170 nm. The fractogram obtained for 600 nm control samples showed a narrow peak eluting at a hydrodynamic diameter of 600 nm. This showed that the extraction method did not influence the particle size distribution. However, the peak of the extracted 600 nm particles (Fig. 3f) shifted towards a smaller hydrodynamic size in comparison to the control 600 nm nanoplastics. The observed shift in the peak of the extracted 600 nm nanoplastics toward the smaller hydrodynamic size compared to the control nanoplastics could result from to the spiking process in which the particles were spiked into the eggshells e.g. due to stirring at pH 9.5 and/or the applied temperature which may lead to degradation of the plastic particles. The second peak appeared in the fractogram of the extracted 600 nm nanoplastics with a hydrodynamic diameter in between 500 and 600 nm. This confirms that the particle spiking method may lead to particle degradation, particularly for larger particles. Similar findings have been previously reported for other type of NM, showing that the NM size distribution varies due to the influence of sample preparation methods on the particles (e.g. Heroult et al., 2014; Abdolahpur Monikh et al., 2018a).

4. Conclusions

In this study, first of all a method have been developed to fractionate and characterize CB-NMs (CNT and nanoplastics) in a NOM suspension mimicking the natural surface water. The developed method could successfully separate the CNT-NOM and nanoplastic-NOM complex from NOM suspension and offers size distribution of the NM-NOM complexes. The NOM influences the size distribution of the CNTs. Second, a stepwise sample preparation method was developed to extract the CNTs and nanoplastics from eggshells with minimum damages to the CB-NMs of interest. The method could not successfully (recovery < 25%) extract the CNTs from eggshells, while it was able to extract the nanoplastics with a high recovery (>60%). The extracted nanoplastics were separated using the developed AF4 method and characterized in

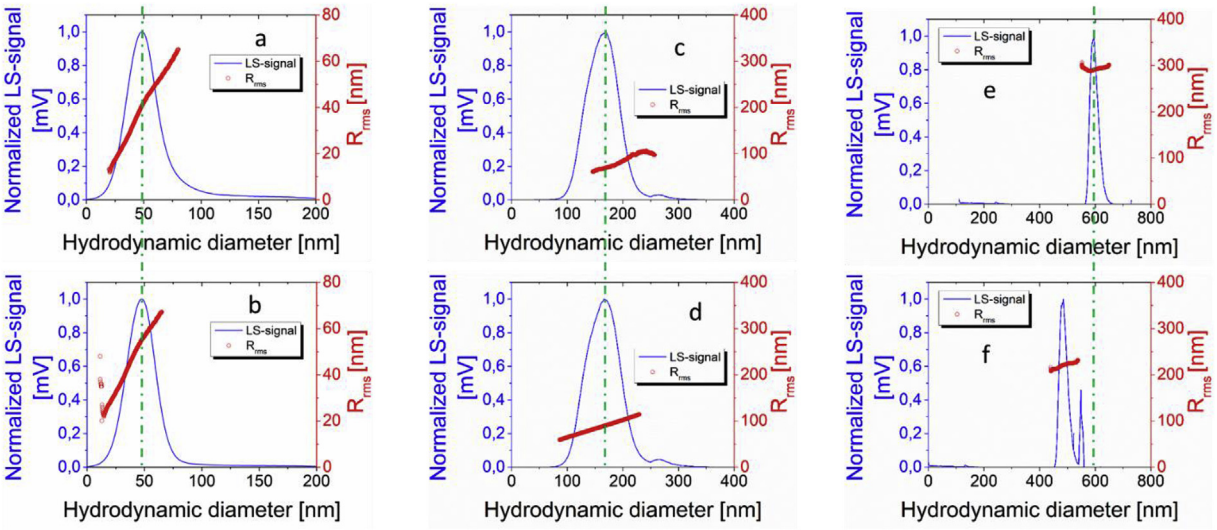

Fig. 3. AF4-MALS fractograms showing the size distribution and R_{rms} of the control and extracted nanoplastics from the eggshells. Control (a) and extracted (b) 60 nm nanoplastics. Control (c) and extracted (d) 200 nm nanoplastics. Control (e) and the extracted (f) 600 nm nanoplastics.

terms of size distribution using MALS. Our findings showed furthermore that the presented methods, extraction followed by AF4-MALS method, did not influence the median size and size distribution of the 60 and 200 nm nanoplastics. A shift was observed in the size distribution of the 600 nm nanoplastics towards a smaller hydrodynamic size. This shift in the particle size could be resulted from the spiking process and not the extraction process because this shift was not detected in the control samples (without spiking process). Our study, thus, demonstrated that there is a potential for applying the developed methods; enabling ultimately the development of a generic sample preparation protocol for characterization of CB-NMs using AF4-MALS. Although homogeneous suspensions of nanoplastics with minimal sample damage can be obtained by the developed methods, more work is required to allow identification of nanoplastics in the samples. The fractions resulting from AF4 are suited for further identification of nanoplastics by using e.g. gas chromatography-mass spectrometry. Nevertheless, we expect that extraction methods and characterization techniques may have to be tailored for a specific nanoplastic.

Acknowledgment

This study was supported by the H2020-MSCA-IF project BTBnano (grant agreement No. 793936).

Appendix A. Supplementary data

Supplementary data to this article can be found online at https://doi.org/10.1016/j.envpol.2019.113304.

References

Abdolahpur Monikh, F., Chupani, L., Vijver, M.G., Vancová, M., Peijnenburg, W.J.G.M., 2019. Analytical approaches for characterizing and quantifying engineered nanoparticles in biological matrices from an (eco)toxicological perspective: old challenges, new methods and techniques. Sci. Total Environ. https://doi.org/10.1016/j.scitotenv.2019.01.105.

Abdolahpur Monikh, F., Chupani, L., Zusková, E., Peters, R., Vancová, M., Vijver, M.G., Porcal, P., Peijnenburg, W.J., 2018a. Method for extraction and quantification of metal-based nanoparticles in biological media: number-based biodistribution and bioconcentration. Environ. Sci. Technol. acs.est.8b03715 https://doi.org/10.1021/acs.est.8b03715.

Abdolahpur Monikh, F., Praetorius, A., Schmid, A., Kozin, P., Meisterjahn, B., Makarova, E., Hofmann, T., von der Kammer, F., 2018b. Scientific rationale for the development of an OECD test guideline on engineered nanomaterial stability. NanoImpact 11, 42–50. https://doi.org/10.1016/j.impact.2018.01.003.

Arenas-Lago, D., Monikh, F.A., Vijver, M.G., Peijnenburg, W.J.G.M., 2019a. Dissolution and aggregation kinetics of zero valent copper nanoparticles in (simulated) natural surface waters: simultaneous effects of pH, NOM and ionic strength. Chemosphere. https://doi.org/10.1016/j.chemosphere.2019.03.190.

Arenas-Lago, D., Monikh, F.A., Vijver, M.G., Peijnenburg, W.J.G.M., 2019b. Interaction of zero valent copper nanoparticles with algal cells under simulated natural conditions: particle dissolution kinetics, uptake and heteroaggregation. Sci. Total Environ. 689, 133–140. https://doi.org/10.1016/j.scitotenv.2019.06.388.

Assemi, S., Newcombe, G., Hepplewhite, C., Beckett, R., 2004. Characterization of natural organic matter fractions separated by ultrafiltration using flow field-flow fractionation. Water Res. 38, 1467–1476. https://doi.org/10.1016/j.watres.2003.11.031.

Au, S.Y., Lee, C.M., Weinstein, J.E., van den Hurk, P., Klaine, S.J., 2017. Trophic transfer of microplastics in aquatic ecosystems: identifying critical research needs. Integr. Environ. Assess. Manag. https://doi.org/10.1002/ieam.1907.

Avio, C.G., Gorbi, S., Regoli, F., 2015. Experimental development of a new protocol for extraction and characterization of microplastics in fish tissues: first observations in commercial species from Adriatic Sea. Mar. Environ. Res. https://doi.org/10.1016/j.marenvres.2015.06.014.

Beckett, R., 2005. Field-Flow Fractionation Handbook. Methods Struct. Anal. protein Pharm.

Benito, A.M., Maser, W.K., Martinez, M.T., 2015. Carbon nanotubes: from production to functional composites. Int. J. Nanotechnol. 2, 71. https://doi.org/10.1504/ijnt.2005.006975.

Bogatu, C., Leszczynska, D., 2016. Transformation of nanomaterials in environment. J. Nanotoxicol. Nanomed. 1, 45–57. https://doi.org/10.4018/jnn.2016010104.

Calzolai, L., Gilliland, D., Rossi, F., 2012. Measuring nanoparticles size distribution in food and consumer products: a review. Food Addit. Contam. A 29, 1183–1193. https://doi.org/10.1080/19440049.2012.689777.

Cano, A.M., Maul, J.D., Saed, M., Irin, F., Shah, S.A., Green, M.J., French, A.D., Klein, D.M., Crago, J., Canas-Carrell, J.E., 2018. Trophic transfer and accumulation of multiwalled carbon nanotubes in the presence of copper ions in Daphnia magna and fathead minnow (Pimephales promelas). Environ. Sci. Technol. 52, 794–800. https://doi.org/10.1021/acs.est.7b03522.

Catarino, A.I., Thompson, R., Sanderson, W., Henry, T.B., 2017. Development and optimization of a standard method for extraction of microplastics in mussels by enzyme digestion of soft tissues. Environ. Toxicol. Chem. https://doi.org/10.1002/etc.3608.

Chen, B., Selegue, J.P., 2002. Separation and characterization of single-walled and multiwalled carbon nanotubes by using flow field-flow fractionation. Anal. Chem. 74, 4774–4780. https://doi.org/10.1021/ac020111b.

Chun, J., Fagan, J.A., Hobbie, E.K., Bauer, B.J., 2008. Size separation of single-wall carbon nanotubes by flow-field flow fractionation. Anal. Chem. 80, 2514–2523. https://doi.org/10.1021/ac7023624.

Cole, M., Lindeque, P., Halsband, C., Galloway, T.S., 2011. Microplastics as contaminants in the marine environment: a review. Mar. Pollut. Bull. https://doi.org/10.1016/j.marpolbul.2011.09.025.

Correia, M., Uusimäki, T., Philippe, A., Loeschner, K., 2018. Challenges in determining the size distribution of nanoparticles in consumer products by asymmetric flow field-flow fractionation coupled to inductively coupled plasma-mass spectrometry: the example of Al2O3, TiO2, and SiO2 nanoparticles in toothpaste.

Separations. https://doi.org/10.3390/separations5040056.
Crawford, C.B., Quinn, B., 2016. Physiochemical properties and degradation. In: Microplastic Pollutants, pp. 57–100. https://doi.org/10.1016/b978-0-12-809406-8.00004-9.
Dehaut, A., Cassone, A.L., Frère, L., Hermabessiere, L., Himber, C., Rinnert, E., Rivière, G., Lambert, C., Soudant, P., Huvet, A., Duflos, G., Paul-Pont, I., 2016. Microplastics in seafood: benchmark protocol for their extraction and characterization. Environ. Pollut. https://doi.org/10.1016/j.envpol.2016.05.018.
Domingos, R.F., Baalousha, M. a, Ju-nam, Y., Reid, M.M., Tufenkji, N., Lead, J.R., Leppard, G.G., Wilkinson, K.J., 2009. Characterizing manufactured nanoparticles in the environment: multimethod determination of particle sizes characterizing manufactured nanoparticles in the environment: multimethod determination of particle sizes. Environ. Sci. Technol. 7277–7284. https://doi.org/10.1021/es900249m.
Doudrick, K., Corson, N., Oberdörster, G., Eder, A.C., Herckes, P., Halden, R.U., Westerhoff, P., 2013. Extraction and quantification of carbon nanotubes in biological matrices with application to rat lung tissue. ACS Nano 7, 8849–8856. https://doi.org/10.1021/nn403302s.
Eatemadi, A., Daraee, H., Karimkhanloo, H., Kouhi, M., Zarghami, N., Akbarzadeh, A., Abasi, M., Hanifehpour, Y., Joo, S.W., 2014. Carbon nanotubes: properties, synthesis, purification, and medical applications. Nanoscale Res. Lett. 9, 393. https://doi.org/10.1186/1556-276X-9-393.
Enders, K., Lenz, R., Beer, S., Stedmon, C.A., 2017. Extraction of microplastic from biota: recommended acidic digestion destroys common plastic polymers. ICES J. Mar. Sci. https://doi.org/10.1093/icesjms/fsw173.
Fimreite, N., Brevik, E.M., Torp, R., 1982. Mercury and organochlorines in eggs from a Norwegian gannet colony. Bull. Environ. Contam. Toxicol. https://doi.org/10.1007/BF01608413.
Freixa, A., Acuna, V., Sanchis, J., Farré, M., Barceló, D., Sabater, S., 2018. Ecotoxicological effects of carbon based nanomaterials in aquatic organisms. Sci. Total Environ. 619–620, 328–337.
Garner, K.L., Keller, A.A., 2014. Emerging patterns for engineered nanomaterials in the environment: a review of fate and toxicity studies. J. Nanoparticle Res. https://doi.org/10.1007/s11051-014-2503-2.
Giddings, C.J., Yang, F.J.F., M.M.N, 1976. Flow field-flow fractionation. field-flow fractionation A versatile a new sep. method, 193, 1244–1245.
Gigault, J., Halle, A. ter, Baudrimont, M., Pascal, P.Y., Gauffre, F., Phi, T.L., El Hadri, H., Grassl, B., Reynaud, S., 2018. Current opinion: what is a nanoplastic? Environ. Pollut. https://doi.org/10.1016/j.envpol.2018.01.024.
Gochfeld, M., Burger, J., 1998. Temporal trends in metal levels in eggs of the endangered roseate tern (Sterna dougallii) in New York. Environ. Res. https://doi.org/10.1006/enrs.1997.3802.
Gogos, A., Kaegi, R., Zenobi, R., Bucheli, T.D., 2014. Capabilities of asymmetric flow field-flow fractionation coupled to multi-angle light scattering to detect carbon nanotubes in soot and soil. Environ. Sci. Nano. https://doi.org/10.1039/c4en00070f.
Hawe, A., Romeijn, S., Filipe, V., Jiskoot, W., 2012. Asymmetrical flow field-flow fractionation method for the analysis of submicron protein aggregates. J. Pharm. Sci. 101, 4129–4139. https://doi.org/10.1002/jps.23298.
Heroult, J., Nischwitz, V., Bartczak, D., Goenaga-Infante, H., 2014. The potential of asymmetric flow field-flow fractionation hyphenated to multiple detectors for the quantification and size estimation of silica nanoparticles in a food matrix characterisation of nanomaterials in biological samples. Anal. Bioanal. Chem. 406, 3919–3927. https://doi.org/10.1007/s00216-014-7831-7.
Hong, S., Elimelech, M., 1997. Chemical and physical aspects of natural organic matter (NOM) fouling of nanofiltration membranes. J. Memb. Sci. 132, 159–181. https://doi.org/10.1016/S0376-7388(97)00060-4.
Hupfeld, S., Ausbacher, D., Brandl, M., 2009. Size characterisation of liposomes using asymmetrical flow field-flow fractionation factors influencing fractionation and size determination. J. Sep. Sci. https://doi.org/10.1002/jssc.200800626.
Hyung, H., Fortner, J.D., Hughes, J.B., Kim, J.H., 2007. Natural organic matter stabilizes carbon nanotubes in the aqueous phase. Environ. Sci. Technol. 41, 179–184. https://doi.org/10.1021/es061817g.
Koh, B., Cheng, W., 2014. Mechanisms of carbon nanotube aggregation and the reversion of carbon nanotube aggregates in aqueous medium. Langmuir 30, 10899–10909. https://doi.org/10.1021/la5014279.
Kowalkowski, T., Sugajski, M., Buszewski, B., 2018. Impact of ionic strength of carrier liquid on recovery in flow field-flow fractionation. Chromatographia. https://doi.org/10.1007/s10337-018-3551-z.
Lambert, S., Wagner, M., 2016. Characterisation of nanoplastics during the degradation of polystyrene. Chemosphere 145, 265–268. https://doi.org/10.1016/j.chemosphere.2015.11.078.
Li, J., Martin, F.L., 2016. Current perspective on nanomaterial-induced adverse effects. In: Neurotoxicity of Nanomaterials and Nanomedicine, pp. 75–98. https://doi.org/10.1016/b978-0-12-804598-5.00004-0.
Loeschner, K., Navratilova, J., Grombe, R., Linsinger, T.P.J., Købler, C., Mølhave, K., Larsen, E.H., 2015. In-house validation of a method for determination of silver nanoparticles in chicken meat based on asymmetric flow field-flow fractionation and inductively coupled plasma mass spectrometric detection. Food Chem. 181, 78–84. https://doi.org/10.1016/j.foodchem.2015.02.033.
López-Heras, I., Madrid, Y., Cámara, C., 2014. Prospects and difficulties in TiO2 nanoparticles analysis in cosmetic and food products using asymmetrical flow field-flow fractionation hyphenated to inductively coupled plasma mass spectrometry. Talanta 124, 71–78. https://doi.org/10.1016/j.talanta.2014.02.029.
López-Miranda, A., López-Valdivieso, A., Viramontes-Gamboa, G., 2012. Silver nanoparticles synthesis in aqueous solutions using sulfite as reducing agent and sodium dodecyl sulfate as stabilizer. J. Nanoparticle Res. 14. https://doi.org/10.1007/s11051-012-1101-4.
Lu, C., Su, F., 2007. Adsorption of natural organic matter by carbon nanotubes. Separ. Purif. Technol. https://doi.org/10.1016/j.seppur.2007.07.036.
Macali, A., Semenov, A., Venuti, V., Crupi, V., D'Amico, F., Rossi, B., Corsi, I., Bergami, E., 2018. Episodic records of jellyfish ingestion of plastic items reveal a novel pathway for trophic transference of marine litter. Sci. Rep. 8. https://doi.org/10.1038/s41598-018-24427-7.
Maser, W.K., Benito, A.M., Martínez, M.T., 2002. Production of carbon nanotubes: the light approach. Carbon N. Y. 40, 1685–1695. https://doi.org/10.1016/S0008-6223(02)00009-X.
Moon, J., Kim, S.H., Cho, J., 2006. Characterizations of natural organic matter as nano particle using flow field-flow fractionation. Colloids Surfaces A Physicochem. Eng. Asp. 287, 232–236. https://doi.org/10.1016/j.colsurfa.2006.05.046.
Moon, M.H., Kang, D., Jung, J., Kim, J., 2004. Separation of carbon nanotubes by frit inlet asymmetrical flow field-flow fractionation. J. Sep. Sci. 27, 710–717. https://doi.org/10.1002/jssc.200401743.
Navrotsky, A., 2010. Thermochemistry of nanomaterials. Rev. Mineral. Geochem. 44, 73–103. https://doi.org/10.2138/rmg.2001.44.03.
Nelms, S.E., Galloway, T.S., Godley, B.J., Jarvis, D.S., Lindeque, P.K., 2018. Investigating microplastic trophic transfer in marine top predators. Environ. Pollut. 238, 999–1007. https://doi.org/10.1016/j.envpol.2018.02.016.
Peters, R.J.B., van Bemmel, G., Herrera-Rivera, Z., Helsper, H.P.F.G., Marvin, H.J.P., Weigel, S., Tromp, P.C., Oomen, A.G., Rietveld, A.G., Bouwmeester, H., 2014. Characterization of titanium dioxide nanoparticles in food products: analytical methods to define nanoparticles. J. Agric. Food Chem. 62, 6285–6293. https://doi.org/10.1021/jf5011885.
Petersen, E.J., Flores-Cervantes, D.X., Bucheli, T.D., Elliott, L.C.C., Fagan, J.A., Gogos, A., Hanna, S., Kägi, R., Mansfield, E., Bustos, A.R.M., Plata, D.L., Reipa, V., Westerhoff, P., Winchester, M.R., 2016. Quantification of carbon nanotubes in environmental matrices: current capabilities, case studies, and future prospects. Environ. Sci. Technol. https://doi.org/10.1021/acs.est.5b05647.
Schmidt, B., Petersen, J.H., Bender Koch, C., Plackett, D., Johansen, N.R., Katiyar, V., Larsen, E.H., 2009. Combining asymmetrical flow field-flow fractionation with light-scattering and inductively coupled plasma mass spectrometric detection for characterization of nanoclay used in biopolymer nanocomposites. Food Addit. Contam. - Part A Chem. Anal. Control. Expo. Risk Assess. 26, 1619–1627. https://doi.org/10.1080/02652030903225740.
Tapasztó, L., Kertész, K., Vértesy, Z., Horváth, Z.E., Koós, A.A., Osváth, Z., Sárközi, Z., Darabont, A., Biró, L.P., 2005. Diameter and morphology dependence on experimental conditions of carbon nanotube arrays grown by spray pyrolysis. Carbon N. Y. 43, 970–977. https://doi.org/10.1016/j.carbon.2004.11.048.
Ter Halle, A., Ladirat, L., Gendre, X., Goudouneche, D., Pusineri, C., Routaboul, C., Tenailleau, C., Duployer, B., Perez, E., 2016. Understanding the fragmentation pattern of marine plastic debris. Environ. Sci. Technol. 50, 5668–5675. https://doi.org/10.1021/acs.est.6b00594.
von der Kammer, F., Legros, S., Hofmann, T., Larsen, E.H., Loeschner, K., 2011. Separation and characterization of nanoparticles in complex food and environmental samples by field-flow fractionation. TrAC Trends Anal. Chem. 30, 425–436. https://doi.org/10.1016/j.trac.2010.11.012.
Wagner, S., Legros, S., Loeschner, K., Liu, J., Navratilova, J., Grombe, R., Linsinger, T.P.J., Larsen, E.H., Von Der Kammer, F., Hofmann, T., 2015. First steps towards a generic sample preparation scheme for inorganic engineered nanoparticles in a complex matrix for detection, characterization, and quantification by asymmetric flow-field flow fractionation coupled to multi-angle light scattering and. J. Anal. Atomic Spectrom. 30, 1286–1296. https://doi.org/10.1039/c4ja00471j.
Welden, N.A., Abylkhani, B., Howarth, L.M., 2018. The effects of trophic transfer and environmental factors on microplastic uptake by plaice, Pleuronectes plastessa, and spider crab, Maja squinado. Environ. Pollut. 239, 351–358. https://doi.org/10.1016/j.envpol.2018.03.110.
Westerhoff, P.K., Kiser, M.A., Hristovski, K., 2013. Nanomaterial removal and transformation during biological wastewater treatment. Environ. Eng. Sci. 30, 109–117. https://doi.org/10.1089/ees.2012.0340.
Yang, K., Xing, B., 2009. Adsorption of fulvic acid by carbon nanotubes from water. Environ. Pollut. https://doi.org/10.1016/j.envpol.2008.11.007.
Zhou, Z., Guo, L., 2015. A critical evaluation of an asymmetrical flow field-flow fractionation system for colloidal size characterization of natural organic matter. J. Chromatogr. A 1399, 53–64. https://doi.org/10.1016/j.chroma.2015.04.035.